Coated boron layers by boronization and a real-time boron coating using impurity powder dropper in LHD

Naoko ASHIKAWA[1, *], Robert LUNSFORD[2], Federico NESPOLI[2], Erik GILSON[2], Yaowei YU[3], Jiansheng HU[3] and Shinichiro KADO[4]

[1]National Institute for Fusion Science, Toki 509-5292, Japan

[2]Princeton Plasma Physics Laboratory, Princeton NJ 08540, United States of America

[3]Institute of Plasma Physics, Chinese Academy of Sciences, Hefei 230031, People's Republic of China

[4]Institute of Advanced Energy, Kyoto University, Kyoto 611-0011, Japan

* E-mail of corresponding author: nasikawa@hotmail.co.jp

Abstract

In Large Helical Device (LHD), diborane (B_2H_6) is used as a standard boron source for boronization, which is assisted by helium glow discharges. In 2019, a new Impurity Powder Dropper (IPD) system has been installed and is under evaluation as a real-time wall conditioning technique. In LHD, which is a large size heliotron device, an additional helium (He) glow discharge cleaning (GDC) after boronization has been operated for a reduction of hydrogen recycling from coated boron layers, and this operational time of 3 h was determined by spectroscopic data during glow discharges. A flat hydrogen profile is obtained on the top surface of coated boron on the specimen exposed to boronization, the result suggests a reduction of hydrogen at the top surface by He-GDC. Trapped oxygen in coated boron was obtained by boronization, and the coated boron, which has boron-oxide, on the first wall by B-IPD was also shown. Considering the difference in coating areas between B_2H_6 boronization and B-IPD operation, it would be most effective to use the IPD and B_2H_6 boronization coating together for optimized wall conditioning.

Keywords: boron layer, oxygen impurity, hydrogen recycling, impurity powder dropper, LHD, EAST

(Some figures may appear in colour only in the online journal)

1. Introduction

Boronization is one of the wall conditioning tools in fusion devices [1–4] as boron coatings are well known for their effect of reducing oxygen impurities due to easily formed chemical compounds such as boron-oxide. In LHD, standard boron coatings are created by boronization, which uses

diborane (B_2H_6) doped helium mixed gasses during glow discharges [5, 6]. Coated areas of boron by boronization are most importantly plasma-facing areas, including first walls and divertor targets. However, as B_2H_6 gas is toxic it requires caution during operation. In 2019, a new impurity powder dropper (IPD) system was installed [7, 8] to be tested as a real-time wall conditioning method. Using the IPD system, amounts and dropped timings of boron powders can be controlled. Due to the application method during active main discharges, the boron layer obtained using the IPD system is mainly considered for divertor targets.

In this paper, characterizations of coated boron layers by boronization and boron-IPD are analyzed. Especially since hydrogen isotope trapping by boron may contribute to wall recycling controls, analytical data of hydrogen isotope is shown. Hydrogen cycling control after boronization by helium glow discharges had been established using the spectroscopic data in LHD. In addition, characterizations of three different boron coating methods, i.e., glow discharge boronization, ion cyclotron wall conditioning boronization, and boron-IPD, are compared in this study.

2. Experimental setup

In LHD, boronization by means of B_2H_6 doped mixed helium (He) glow discharge has been operated. In the early boronization in LHD, the gas was introduced from one port at the 1.5 lower section. After that, the introduction of gas increased to three ports from 2002. In EAST, at the beginning of the project, boronization was carried out by using $C_2B_{10}H_{12}$ [9]. In addition, the ion cyclotron wall conditioning (ICWC) [3, 4, 9] has been used for steady wall conditioning in EAST, and the method of adding $C_2B_{10}H_{12}$ gas to the He-ICWC discharge was also implemented to apply a boron coat. Details on operations are given in reference [10] or section 3.

Material manipulators are installed on both LHD and EAST. In LHD, the material manipulator located in the 4.5 lower port was used, with the surface of specimens located at the first wall position in this work. The location of the material manipulator is shown in figure. The material manipulator is separated by the vacuum gate valve between the plasma vacuum vessel and the manipulator, and up/down movement is controlled by the remote system. During the boronization operation, material exposure experiments can be performed by remote control, even entry into the torus hall is not possible due to the toxicity of B_2H_6 gas.

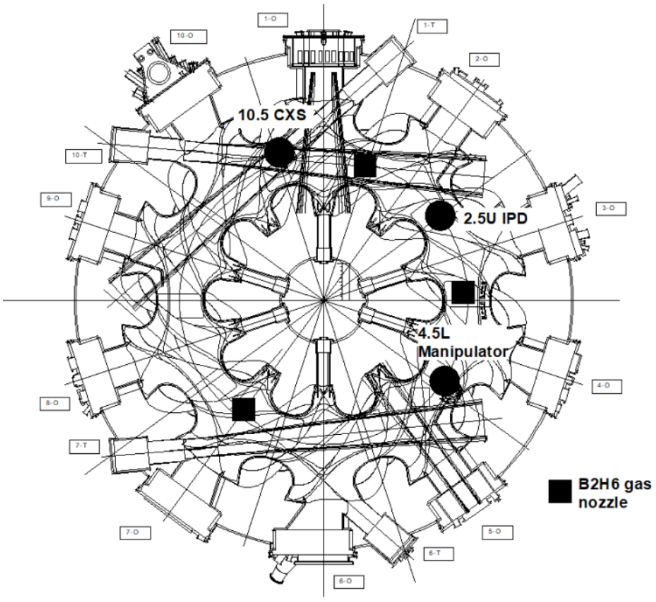

Figure 1. Schematic drawing of locations for IPD at the 2.5 upper port, the material manipulator at the 4.5 lower port, charge exchange spectroscopy (CXS) at the 10.5 and gas injection nozzles of B_2H_6 at the 1.5 lower, 3.5 lower, 7.5 lower ports in LHD.

In EAST, the manipulator was located at the midplane of a low field side. The manipulator that had a small head of about 5 cm was used, and the manipulators were installed when required for an experiment. The manipulator is also separated between the plasma vacuum vessel and the manipulator by the vacuum gate valve. However, the movement of the head with specimens to the plasma vacuum area was required manually. Therefore, the head was installed at the first wall position before inserting B_2H_6 gas. When samples are removed from the head of manipulators, specimens are exposed to the atmosphere, and their top surface is oxidized in both manipulators in LHD and EAST. However, the oxidizing effect of the atmosphere is known from previous studies [6].

The IPD system is installed at the 2.5 upper port in LHD, as shown in figure 1. Two compositions, boron (B) and boron nitride (BN) powders can be used, at present [7]. A powder dropping rate and an operational period are controlled by a piezo element and the typical flow rate is about 0.1–0.5 mg/s in this experiment. During the IPD experiment, the manipulator at the 4.5 lower port was used in LHD, and the details of analytical data are shown in section 3.

Two kinds of surface analyses are used; glow discharge optical emission spectroscopy (GD-OES) is used for depth profiles of compositions as qualitative analyses with argon (Ar) as the working gas and X-ray photoelectron spectroscopy (XPS) is utilized to obtain the depth profiles of atomic concentrations. XPS measures the chemical bindings of compositions. GD-OES measures elements from hydrogen to high-Z materials. The GD-OES used in this study can measure hydrogen and deuterium separately. Target specimens and their history are written in table 1. More details of these

specimens are discussed in section 3.

Table 1. Target specimens and their experimental histories.

Name	Device	Base material	Boron coating		Additional plasma exposure	
Sample B1	EAST	Si	$C_2B_{10}H_{12}$ by ICWC	First wall position		
Sample B2	LHD	SS316	B_2H_6 by GDC	First wall position		
Sample B3	LHD	SS316	B power during H plasma	First wall position		
Sample B4	LHD	SS316	B_2H_6 by GDC	First wall position	About 20 D plasma discharges	First wall position

3. Results and discussions

3.1. Characterizations of three boron coating methods

First, based on the EAST and LHD experiments, table 2 shows the characteristics of the following three boron coatings. (1) $C_2B_{10}H_{12}$ and He mixing gas during ICWC operation, (2) B_2H_6 gas and He mixing gas during glow discharge, (3) Boron powder droppings during the main plasma discharge.

Table 2. Characterizations of three boron coating methods.

	Boronization: EAST	Boronization: LHD	Boron dropping: LHD
Working gas / conditioning plasma and these number of systems	Carborane ($C_2B_{10}H_{12}$)+He / ICWC	Diborane (B_2H_6) + He / GDC	Boron powder (Diameter: 150 μm)
	1 (ICR antenna)	2 (GDC anode)	(main plasma)
	1 s on / 2 s off		
Number of gas injection or dropping port	1	3	1
Material of first wall / divertor	Mo / doped Graphite	SUS316 / Graphite	SUS316 / Graphite
Wall temperature	Room temperature	Room temperature	Room temperature
C : O : B （XPS）	3 : 1 : 6	1 : 2 : 7 [6]	No data
Operational characterizations	･Conditioning plasma, under confinement magnetic fields	･Conditioning plasma, no magnetic field	･Real-time boron coating under strong confinement magnetic fields
	Affecting areas by ICWC are surfaces on divertor and first wall, which are having line of sights from plasmas [11]. But the area is limited to compare with GDC	･Most widely coated boron is obtained on divertor and first wall	･Coating area is the first wall (in this work) and might be divertor
	･Injected B amounts: 10g (in $C_2B_{10}H_{12}$)	･Injected B amounts: 37g (in B_2H_6)	･Dropped B powder: about 800 mg
Types of coated boron layer	･High carbon concentration is observed in the boron layer. Boron formed a binding with carbon in the coated layer. ･The layer formed an effective boron-oxide and It was confirmed that trapped oxygen in the boron layer.	･Thick boron layer of 100–1000 nm was obtained per one boronization. ･High purity of boron layer can be possible, and the pure boron affected additional oxygen trapping after boronization, such as main discharges.	･On the first wall, thin boron coating is obtained and hydrogen as working gas of main plasmas and oxygen are trapped in the layer during a process of boron coating.

The most crucial point is the limitations and conditions regarding the operations of boronization methods. GDC and ICWC are applied during conditioning plasmas, while the IPD is operated during the main discharge. GDC is operated without magnetic fields, but ICWC and IPD are operated under

magnetic fields. Thus, differences in base plasmas lead to different coated areas. Boron trapping efficiencies for hydrogen isotopes and oxygen by chemical bindings in the boron layer are well known, however real-time interactions and trappings between boron and other compositions are still under discussion. One of the candidate ideas is the interaction between boron powder and edge plasmas around the divertor regions based on spectroscopic observations [12].

The real-time interactions by boron can be operated by the IPD method only, and it is a unique technique, even in future fusion devices. The results of the new analysis data are described after section 3.2.

3.2. Reduction of remained hydrogen after boronization in LHD

Figure 2 shows time of hydrogen alpha (H_α) emission measured by visible spectroscopies, which was the charge exchange spectroscopy (CXS) [13] at upper and lower ports of the 10.5 port in LHD. H_α intensities over (a) 4 h and (b) totally 59 h as measured by the visible spectroscopies versus an elapsed time from 16:00, which is time = 0 min in figure 2, on January 12, 2002, are shown. In the boronization, flow of B_2H_6 gas begun to decrease at 15 min, and a closing time of the B_2H_6 gas injection was 24 min. Arrows in figure 2 show the operational time of a helium (He) GDC, which was continuously operated from the whole boronization process.

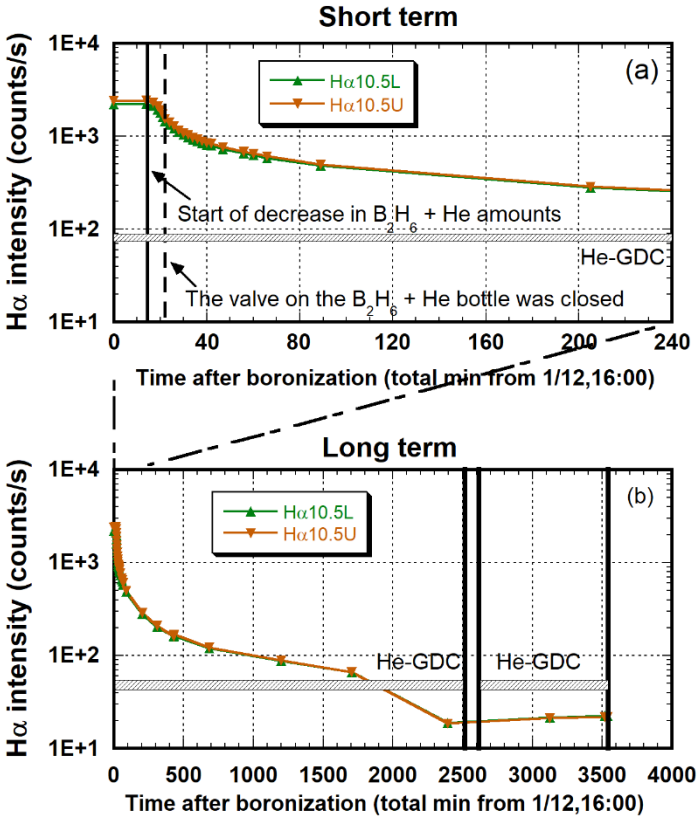

Figure 2. H_α intensities were measured by visible spectroscopy of CXS for (a) 4 h and (b) 59 h.

The optical fibers connected to spectrometers were located at the 10.5 upper and lower ports, and an electric anode for the glow discharge was located at the midplane of the 10.5 section, in the plasma vacuum vessel. A B_2H_6 gas nozzle at the 1.5 lower port was used in the LHD experimental campaign. Two sets of the visible spectrometers were located close to the anode of glow discharge and B_2H_6 gas injection nozzle. Intensities of H_α emission during glow discharges are uniform at different optical fiber lines on the cross-section of the viewport, therefore intensities at the lower and upper spectrometers are approximately equivalent to each other.

A reduction of H_α intensity was observed continuously 15 min until the end of He-GDC, the most significant reduction of H_α was in the first 3 h. After 24 min, a reducing the hydrogen, as observation of H_α, production by the separation between B and H in B_2H_6 gas occurred. However, a continuous decrease in hydrogen was still observed. The reason for this is thought to be that the hydrogen contained on the surface of the boron film coated on the plasma-facing wall was desorbed by the sputtering of the He glow discharge. The coated boron by boronization has an advantage of oxygen reduction and a disadvantage of higher recycling toward next day's plasma experiments, especially when plasma experiments with low electron density are required, in general. A result in figure 2 shows the useful method of hydrogen reduction after boronization, which became the current operational scenario, additional He-GDC of 3 h after a stop of B_2H_6 gas injection, in LHD. Hydrogen recycling effects of coated boron on specimens are discussed in section 3.3.

3.3. Depth profiles of coated boron layers in boronization and boron dropping by IPD

Figure 3 shows depth profiles of compositions on specimens measured by GD-OES. Figures 3(a), (c), and (e) show the normalized intensities of carbon, calculated by dividing the deposited carbon intensities on the target specimens by the intensity obtained on the graphite standard sample, IG-430U. The normalized carbon amounts are over 1 at the top surface of the specimens. However, the top surface is influenced by air contamination, including carbide, and is not included in this discussion.

The boundary between the coating layer and the base specimens was determined as half intensities of materials for base specimens, which is iron (Fe) as the main component of stainless steel (SS) 316 or silicon (Si), and is shown by dashed lines. Figure 3(a) shows higher intensities of normalized carbon as compared with the cases shown in figures 3(c) and (e), due to carbon content of the working gas, $C_2B_{10}H_{12}$, with the profile of the normalized carbon displaying higher intensity at the top surface of the coated B layer, and a decrease in signal deeper from the top surface.

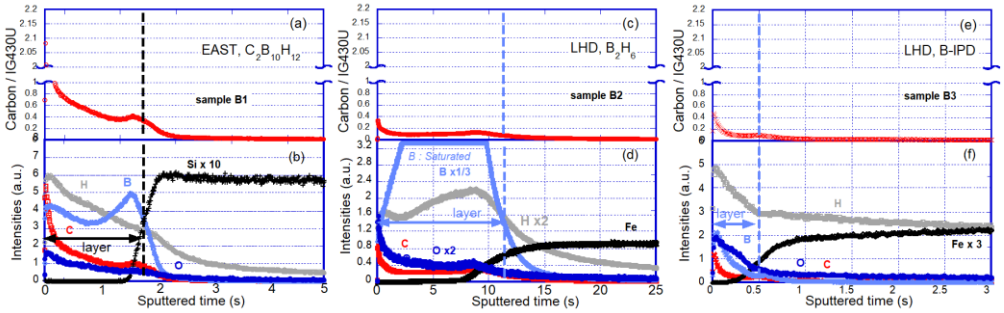

Figure 3. Depth profiles of compositions on specimens measured by GD-OES. (a) and (b) Silicon specimens, sample B1, exposed to $C_2B_{10}H_{12}$ boronization in EAST, (c) and (d) a stainless steel 316 specimen, sample B2, exposed to B_2H_6 boronization in LHD, (e) and (f) a stainless steel 316 specimen, sample B3, exposed to hydrogen plasmas with boron (B) powder dropping by IPD in LHD. Figures 3(a), (c), and (e) show the normalized intensities of carbon, calculated by dividing the deposited carbon intensities on the target specimens by the intensity obtained on the graphite standard sample, IG-430U.

In figure 3(b), which is the same specimen in EAST experiment for figure 3(a), depth profiles of hydrogen and oxygen intensities are similar to carbon's profile, such as reducing intensities toward deeper regions. In addition, carbon is clearly remained into boron layer of EAST. Higher hydrogen recycling after a boronization which used $C_2B_{10}H_{12}$, was observed and it is a disadvantage of their plasma operations in EAST. A profile of hydrogen with higher intensity at the top surface of the coated boron layer is considered to relate to higher hydrogen recycling, such as shown in figure 3 (b).

In figure 3(d), a depth profile of hydrogen intensity shows from the top surface to an interface in a coated boron layer in LHD. A gradual decrease was observed from t = 8 s to 0 s as the sputtered time, and it is considered that higher remained hydrogen at the top surface was removed by He-GDC after the boronization. This surface analysis data shows consistent with the trend of CX data for the 3 h of additional He-GDC shown in figure 1, which is effective in reducing hydrogen recycling.

Figure 3(f) shows a coated boron layer by boron powder dropping with a diameter of 150 μm, during hydrogen plasmas of IPD experiments on December 3 and 6 in 2019. An SS316 specimen was exposed to hydrogen plasmas using the material manipulator at the 4.5 lower port. Surfaces of the specimens were set at the first wall position during boron powder IPD experiments. Total amount of dropped boron powders is about 800 mg. This experiment uses strong magnetic fields to confine plasmas, therefore the coating on divertor targets was expected, but transport to the first wall was unknown. From a coated boron profile in figure 3(f), it is clearly shown that a boron coating from the IPD at the 2.5 section was deposited on the first wall at different toroidal section, namely the 4.5 section, as shown in figure 1.

The changes in the depth profiles for hydrogen and oxygen are similar to each other in the coated boron layer. Therefore, it is considered that hydrogen and oxygen were trapped in boron layer formation. An advantage of B-IPD is that real-time interactions occur during the main plasma discharges, however, the extent of a longer lifetime of the coated layer is not clear. But it is not a serious issue as the limitation regarding operational time of IPD is negligible to compare with boronization.

3.4. Chemical bindings of coated boron layers

Figure 4(a) shows a depth profile of atomic concentrations for a coated boron layer, in which the specimen, sample B1, exposed to ion cyclotron wall conditioning boronization with $C_2B_{10}H_{12}$ of EAST, was measured by XPS. A coated thickness of the boron layer is about 45 nm, with the depth position determined by 50% of Si as a base specimen. The coated layer is comprised of 60% boron, 30% carbon, and 10% oxygen. Carbon concentration in the layer is higher than that in the coated boron layer in LHD [6], reasonably considering the presence of carbon in $C_2B_{10}H_{12}$.

Narrow profiles for boron, oxygen, and carbon on sample B2 are analyzed, as shown in figures 4(b)–(d). The observed thickness of EAST boron layer of about 34 nm as a hatched line, F4, is shown using XPS with Ar ion sputtering in figure 4(a). In figures 4(b)–(d), the observed thickness of LHD boron layer is about 14 nm from the top surface, measured by XPS. A depth profile for the specimen, sample B2, of LHD is presented in reference [6]. In figure 4(b), the large amount of B-O binding in the LHD boron layer is shown. In figure 4(c), Highly Oriented Pyrolytic Graphite (HOPG) was measured to obtain a standard peak of C–C. The EAST boron layer shows a combination between C–C and C–B, and the LHD boron layer shows mainly a C–B peak, as shown in figure 4(c).

From fitting analyses for the area separation of B–B, B–C, and B–O bindings as shown in the peak positions of the boron narrow profile in figure 4(d), chemical compositions and concentrations for B–B (188.2 eV), B–C (189.5 eV), and B–O (192.0 eV) [14], in the B1s peak of EAST and LHD layers are analyzed, as shown in table 3. EAST boron shows mainly boron-carbide (B–C) of 70%. The remaining amount of boron is observed as boron oxide (B–O) and then pure boron was negligible in the layer of EAST. In LHD, pure boron as B-B still remains in the layer, and other bindings are B–O and B–C. When pure boron is facing to plasmas after a sputtering by discharges such as GDCs or main plasma discharges, the top surface of pure boron can trap impurities [6]. Hence, the concentration of pure boron remaining in the boron layers is important in the point of impurity reduction. It should also be noted that the top surface is changed by these sputtering processes.

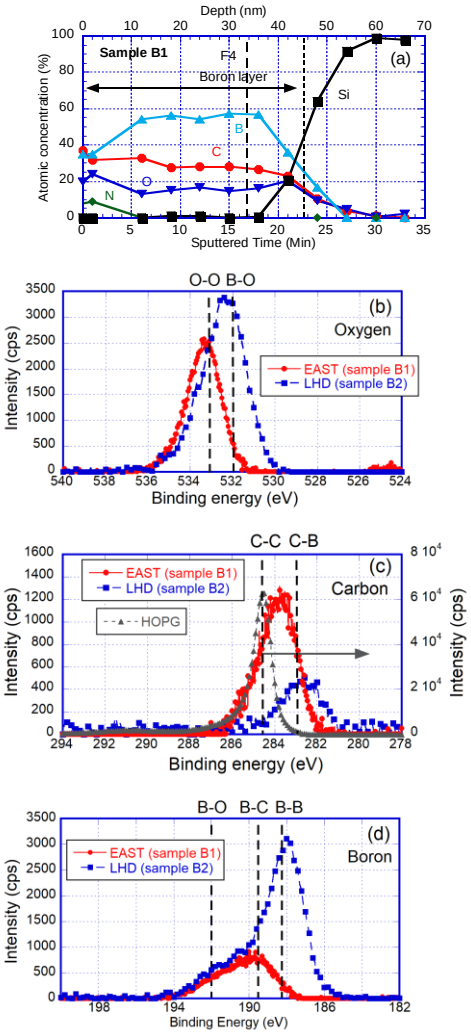

Figure 4. (a) XPS measured the depth profile of atomic concentrations for the coated boron layer on a specimen exposed to boronization using $C_2B_{10}H_{12}$ in EAST. Narrow profiles of (b) oxygen, (c) carbon, and (d) boron in coated boron layers obtained from LHD [6] and EAST boronization. In figure 4(c), HOPG is used as a standard graphite sample.

Table 3. Chemical composition and concentration of coated boron layers in EAST and LHD.

	B-B (%)	B-C(%)	B-O (%)
EAST ($C_2B_{10}H_{12}$)	--	70	30
LHD (B_2H_6)	65	19	16

3.5. Interaction between hydrogen and coated boron layer

In figure 5, an SS316 specimen, namely sample B2, was exposed to boronization (B_2H_6) in the

plasma vacuum vessel of LHD using the material manipulator and subsequently removed. One of the specimens after LHD boronization was exposed to deuterium main plasma discharges of about 20 shots at a later date at the first wall position using the material manipulator, and data of the specimen, namely sample B4, is also shown.

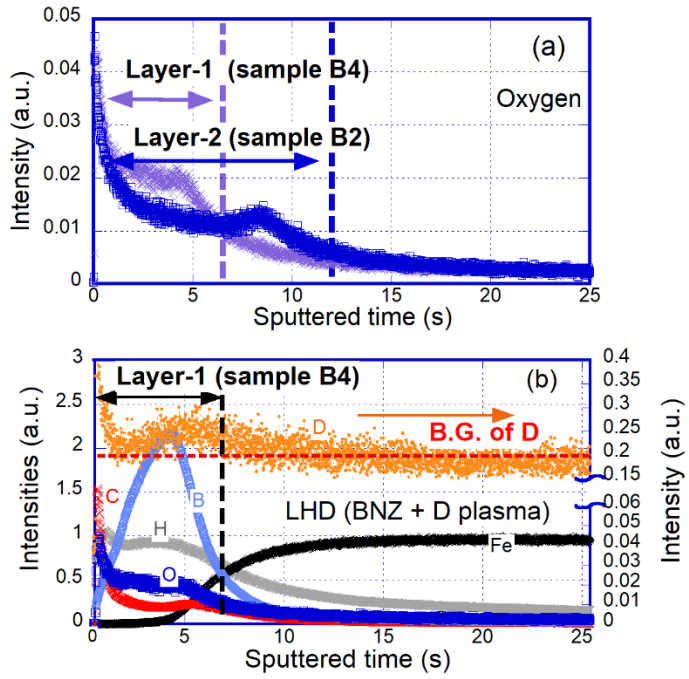

Figure 5. (a) Depth profile of oxygen intensities on coated boron layer, Layer-2, on sample B2, which layer is obtained after boronization. Originally, sample B4 had a boron layer by boronization, as shown in Layer-2. However, it was exposed to deuterium plasmas, which eroded the boron layer, and the remaining thickness of the boron is shown as Layer-1. (b) Compositions and deuterium (D) intensities on sample B4 were measured by GD-OES. A dotted line shows a background (B.G.) level of deuterium intensity.

For both types of specimens with and without deuterium plasma exposures, oxygen intensities measured by GD-OES are compared, as shown in figure 5(a). A thickness of coated boron with deuterium main plasmas is thinner than that of coating without plasma exposures, indicating that the coated layer was eroded by main plasmas. Intensities of oxygen in coated boron layer with deuterium main plasmas are higher than those without plasma exposures. Therefore, the efficiency of oxygen trapping to the top surface of coated boron is shown in figure 5(a).

Figure 5(b) shows intensities of compositions on boron layer after boronization with plasma exposures on sample B4. An intensity of boron at the surface shows a reduction, and a peak of boron shows into the coated layer. The deuterium depth profile shows higher intensity at the top surface of the coated boron layer. An interaction with hydrogen isotopes on the coated boron layer has been reported to have the effect of shielding for hydrogen isotope permeations [15], and it is also considered

that deuterium produced by main plasma discharges is retained only on the top surface of the coated layer. Therefore, comparing figures 5(a) and (b) clearly shows a difference in the trapping depth of oxygen and hydrogen after plasma exposures in the boron layers.

Thus, section 3 presents comprehensive characterizations of coated boron layers using surface analyses. Considering the difference in coating areas between B_2H_6 boronization and B-IPD operation, better operational scenarios may be obtained when these two techniques are used together.

4. Conclusions

Two boron coating methods, boronization as a wall conditioning and real-time boron coating by IPD, are operated in fusion devices, and their characteristics are summarized in this work.

In LHD, a time evolution of reduction for hydrogen as a higher recycling source from the coated boron layer was observed. It was found that sufficient reduction of hydrogen was achieved after stopping B_2H_6 gas injection by carrying out a 3 h He-GDC. Now, it has become the standard operational scenario in LHD.

Different types of coated boron layers, operated by $C_2B_{10}H_{12}$ by He-ICWC, B_2H_6 by He-GDC, and B-IPD, are discussed. It was clarified that the top surface of the boron layer also contributes to oxygen trapping during the main discharges. A comparison of coated boron between $C_2B_{10}H_{12}$ and B_2H_6 is shown, and the coated boron layer using $C_2B_{10}H_{12}$ shows indications of chemical bindings with carbon. Thus, the remaining high-purity boron layers are limited when compared with the boron layer by B_2H_6. It was revealed that the purer boron remains, the more oxygen impurities are trapped in the subsequent main discharges. Hence, the concentration of pure boron remaining in the boron layers is important for impurity reduction.

It was shown that a thin boron layer was coated on the first wall by B-IPD experiments, and material analysis revealed the effect of trapping oxygen and hydrogen at the top surface of the coated boron layer. Boron coating by B-IPD during the main discharge is considered to be more effective on the divertor region. However, this part was not evaluated in this experiment due to restrictions on using the manipulator. More details of real-time interactions between hydrogen isotopes and boron are discussed in future works. Considering the difference in coating areas between B_2H_6 boronization and B-IPD operation, better operational scenarios may be obtained when these two techniques are used together.

Currently, only B_2H_6 can be produced in East Asia as a source of deuterated boron. JT-60SA plans to use B_2D_6 for their boronization. ITER starts a discussion for additional wall conditioning, including boron coatings, relating to changing the first wall materials from beryllium to tungsten. Hence, it is

important to understand the characteristics of coated boron walls.

Acknowledgments

This work is supported by NIFS budgets, KOBF031, ULFF004 and KUHR032. This research was partly supported by JSPS KAKENHI 18K04999, JSPS-CAS Bilateral Joint Research Projects, "Control of wall recycling on metallic plasma facing materials in fusion reactor" 2019–2022, (No. GJHZ201984), Chinese Academy of Sciences President's International Fellowship Initiative Grant No.2024VMB0003 in FY2023 and U.S. Department Of Energy under Contract No. DE-AC02-09CH11466 with Princeton University.

An author (Naoko Ashikawa) wants to thanks to Dr. Mamoru Shoji (NIFS) for operational supports of the material manipulator in LHD, Mr. Junichi Yagyu (QST) for useful discussions about boronization, Dr. Hyungho Lee (Korea Institute of Fusion Energy, Republic of Korea) for a kindly support about an optical fiber procurement for IPD, and Dr. Volker Rohde (Max Planck Institute for Plasma Physics, Germany) for useful advice about hardware settings of IPD in tokamak/helical hall.

References

[1] Winter J 1996 P*lasma Phys. Control. Fusion* **38** 1503
[2] Yagyu J *et al* 1997 *J. Nucl. Mater.* **241-243** 579
[3] Gu X M *et al* 2000 *J. Plasma Fusion Res. Ser* **3** 320
[4] Li J G *et al 2000 J. Plasma Fusion Res. Ser* **3** 40
[5] Nishimura K *et al* 2003 *J. Plasma Fusion Res.* **79** 1216
[6] Ashikawa N *et al* 2007 *J. Nucl. Mater.* **363-365** 1352
[7] Nespoli F *et al 2020 Nucl. Mater. Energy* **25** 100842
[8] Lunsford R *et al* 2022 *Nucl. Fusion* **62** 086021
[9] Wu J H *et al* 2011 *J. Nucl. Mater.* **415** S1046
[10] Hu J S *et al* 2009 *Fusion Eng. and Des.* **84** 2167
[11] Ashikawa N *et al* 2011 *J. Plasma Fusion Res.* **6** 2402138
[12] Kawate T *et al* 2022 *Nucl. Fusion* **62** 126052
[13] Ida K *et al* 2001 *Rev Sci. Inst.* **71** 2350
[14] Hu T *et al* 1998 *Thin Solid Films* **332** 80
[15] TsuzukiK *et al* 1997 *J. Nucl. Mater.* **241-243** 1055